PAPER

Check for updates

A poly(allylamine hydrochloride)/poly(styrene sulfonate) microcapsule-coated cotton fabric for stimulus-responsive textiles

Zhiqi Zhao,[ab] Qiujin Li, [ID] *[ab] Jixian Gong,*[ab] Zheng Li[ab] and Jianfei Zhang[abc]

This study reports the design of a stimulus-responsive fabric incorporating a combination of microcapsules, containing polyelectrolytes poly(allylamine hydrochloride) (PAH) and poly(styrene sulfonate) sodium salt (PSS), formed *via* a layer-by-layer (LBL) approach. The use of PAH and PSS ensured that the microcapsule structure was robust and pH-sensitive. SEM and TEM studies showed that the composite microcapsule $(PAH/PSS)_nPAH$ had a spherical morphology with a hollow structure. FTIR demonstrated the presence of PAH and PSS, confirming the composition of the microcapsule shell. DSC showed that the microcapsules were thermally stable. The size of the microcapsules ranged from 4 μm to 6 μm. The hollow microcapsules can be used as a carrier for loading and releasing chemicals under different pH conditions. The release rate of Rhodamine-B from $(PAH/PSS)_nPAH$ microcapsules was higher at pH 5.8 than that at 7.4, confirming the pH sensitivity. The hollow structure of $(PAH/PSS)_nPAH$ microcapsules is expected to act as a carrier and medium to introduce functional chemicals into the fabric with long-lasting property and pH stimulus responsivity. Furthermore, a positively charged compound with ethylene oxide groups was added during the coating process as a crosslinker binding $(PAH/PSS)_2PAH$ for the microcapsules with the cotton fabric more efficiently. Using this method, numerous substances, *e.g.*, drugs, dyes, natural herbs, or perfumes, could be stored into the LBL microcapsules for a relatively long time, constantly releasing them from the coated textiles. Since LBL microcapsules were easy to combine with fabrics, this study provided a feasible approach for the preparation of functional stimulus-responsive textiles.

1 Introduction

Stimulus-responsive polymers are a group of intelligent materials, some of which can self-assemble *via* a physical or chemical process in response to small external changes in the environment. pH-responsive polymers can respond to the pH of the surrounding environment by undergoing structural and property changes, and they have gained a great deal of intensive academic and commercial interests in recent decades owing to their wide-span application potentials in pollutant control and treatment,[1,2] controlled-release systems,[3,4] drug delivery systems[5,6] and other biotechnological applications.[7,8] In general, by combining stimulus-responsive polymers with fabrics, stimulus-responsive textiles can be prepared. It is important that the affinity and interactions between the fabric and

stimulus agent as well as the lasting property of the modified textile are of utmost concern. Through forming membranes, an emulsion or suspension immersion, coatings, *etc.*, stimulus agents can be combined with fabrics. Stimulus-responsive textiles have consequently emerged as an important category of functional materials, providing various applications as self-repairing materials, textile sensors[9,10] and drug delivery materials.[11] Different stimulus have been employed to drive these intelligent textiles, including pH,[12] temperature,[13,14] and electric[15] and magnetic fields.[16,17]

Microcapsule modifications that seal various ingredients within small vectors that can easily be combined with textile fibers have been widely studied in several fields on the basis of their controlled release and delivery properties.[18,19] Based on the current global environmental situation, clean chemistry protocols are much preferred as one of the most essential requirements for scientific and technological developments. Nevertheless, most of the commercial microcapsules already used in textile materials are manufactured from melamine-formaldehyde, phenol-formaldehyde resins, *etc.*, which can be potentially hazardous to environmental safety, because of the toxicity of formaldehyde.[20] Consequently, finding milder materials and approaches are becoming increasingly important.

[a]School of Textile Science and Engineering, Tiangong University, Tianjin 300387, China. E-mail: vicmaldini@126.com; gongjixian@126.com; Tel: +86-18622272697; +86-18920787809

[b]Key Laboratory of Advanced Textile Composites, Ministry of Education, Tiangong University, Tianjin 300387, China

[c]Collaborative Innovation Center for Eco-Textiles of Shandong Province, Qingdao 266071, Shandong, China

Because of their advantages, such as benign preparation conditions, controllable particle size and designable shell formation components, layer-by-layer prepared microcapsules have been widely used in pharmaceutical engineering,[21,22] food engineering[23,24] and tissue engineering.[25,26] Through a layer-by-layer method, some agents can be used as the blocks to form microcapsule shell, *e.g.*, polyelectrolytes with opposite charges.[27,28]

In the past years, polymers prepared by the LBL technology have developed rapidly. As published by Raichur *et al.*, poly (allylamine hydrochloride) (PAH) and poly (methacrylic acid) (PMA) were assembled *via* a layer-by-layer method to form a polyelectrolyte multilayer (PEM), which can be used as the self-reaction film platform for transdermal drug delivery, an antibacterial or anti-inflammatory coating for implants, and drug release coating for scaffolds.[29] Sukhorukov *et al.*, prepared a drug carrier with a good sustained release through an LBL assembly of PAH and polystyrene sulfonate (PSS), improving the clinical application effect in medical and dental fields.[30] In our previous study,[31] low-magnetization magnetic microcapsules were formed by PAH and superparamagnetic iron oxide (SPIOs) *via* the LBL technique. These magnetic microcapsules were employed as a synergistic theranostic platform for remote cancer cell therapy and served as drug delivery, hyperthermia and magnetic resonance imaging (MRI) contrast agents simultaneously. Some composites prepared through electrostatic interactions between oppositely charged polyelectrolytes are pH[32-34] or temperature[35-37] sensitive, such as microcapsules and nano hydrogels. These composites are supposed to be suitable carriers for loading chemicals and then be bonded to fabrics, generating functional textiles. Moreover, with the changes in the surrounding environment (*e.g.*, pH or temperature), the functional chemicals would be released controllably, generating stimulus-responsive functional textile.[38] Pourjavadi *et al.* prepared polyisopropylacrylamide (PNIPAAm)/chitosan (PNCS) nano hydrogels containing cinnamon oil to modify cotton fabrics, yielding functional textile with temperature-responsive antibacterial property.[39] Wang *et al.* studied the cellulose/silica composite microcapsules used as finishing agents yielding waterborne multifunctional fabrics with the controllable release properties of lavender essential oil.[40] In view of its stimulus-responsive applications in textiles, pH-stimulus sensitive microcapsules are usually coated on pure cotton fabrics known as the suitable materials for direct contact with the human skin because the weak acid solution environment (pH 4.5–6.5) provided by sweat[41,42] would trigger the controlled release of the chemicals from the microcapsules.

This study presents a type of stimulus-responsive textile coated with self-assembled microcapsules made of poly(allylamine hydrochloride) (PAH) and poly(styrene sulfonate) sodium salt (PSS) *via* the layer-by-layer (LBL) technique. The hollow structure of the (PAH/PSS)$_n$PAH microcapsules is envisioned to be the carrier and medium to introduce some functional chemicals, *e.g.*, drugs or perfumes to form fabrics with the long-lasting property. Besides, since the electrostatic interactions

between PAH and PSS is sensitive to pH, this (PAH/PSS)$_n$PAH microcapsule-coated fabric can be employed as a pH stimulus-responsive textile, releasing functional chemicals with the changes in the surrounding environment. Due to the rare allergic reactions associated with cotton, combining layer-by-layer microcapsules with cotton fabric can generate a functional textile that can have direct contact with the skin.

2   Experimental section

2.1   Materials

Poly(allylamine hydrochloride) (PAH), poly(styrene sulfonic acid) sodium salt (PSS $M_w \approx 70$ kDa) and Rhodamine-B (RhB) were purchased from Alfa Aesar (Tianjin) Co., Ltd. Ethylenediaminetetraacetic acid (EDTA) was purchased from Beijing Puboxin Biotechnology Co., Ltd, and the other reagents were of analytical grade. Standard 100% cotton fabric (weight 106.6 g m^{-2}, warp 133 yarns per inch, weft 72 yarns per inch, and thickness 0.21 mm) was bought from Tianyi printing and dyeing company in Tianjin, China.
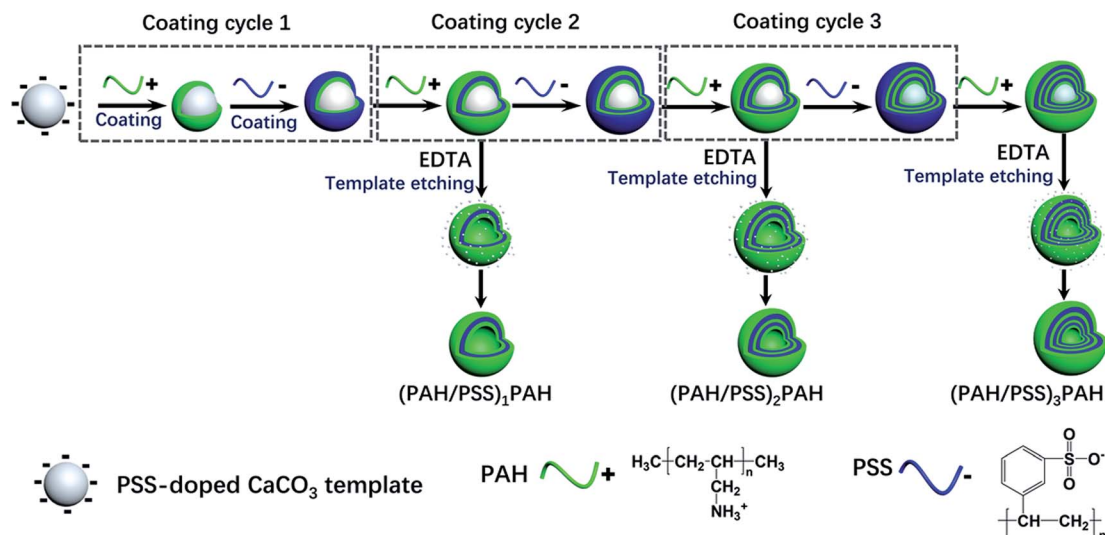
2.2   Preparation of (PAH/PSS)$_n$PAH microcapsules

A Ca(NO$_3$)$_2$·4H$_2$O solution (100 mL, 0.025 M) consisting of PSS (200 mg) was rapidly poured into an equal volume of Na$_2$CO$_3$ (100 mL, 0.025 M) under stirring for 10–20 s. After maintaining for 15–30 min, the precipitated PSS-doped CaCO$_3$ particles were washed with de-ionized water and collected. The PSS-doped CaCO$_3$ templates were dispersed into the PAH solution (10 mL, 1.0 mg mL^{-1}, 0.5 M NaCl) for 15 min under continuous shaking. The resulting particles were washed 3 times with de-ionized water and collected through centrifugation (7000 rpm for 1 min). Then, the coated particles were incubated in a PSS solution (10 mL, 1.0 mg mL^{-1}, 0.5 M NaCl) following the same procedure (a coating cycle, shown in Scheme 1). The multilayer structure was formed by an alternating assembly of corresponding materials (repeated the coating cycles). The hollow microcapsules were obtained through the etching of CaCO$_3$ templates using the EDTA solution (30 mL, 0.1 M, pH 7.0). The process is shown in Scheme 1.
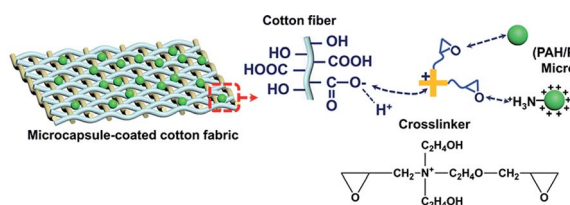
2.3   Characterization of (PAH/PSS)$_n$PAH microcapsules

The size of PSS-doped CaCO$_3$ particles was determined by a diffraction method using a laser analyzer (Horiba LA-300). The morphology of the (PAH/PSS)$_n$PAH microcapsules was determined using a scanning electron microscope (SEM) (Hitachi S4800, HITACHI) at an accelerating voltage of 20 kV, transmission electron microscope (TEM) (Hitachi H7650, HITACHI) operated at 120 kV and ultra-depth-of-field three-dimensional microscope (VHX-1000, KEYENCE). Fourier transform infrared spectroscopy (FTIR) was performed using a Nicolet is 50 (Thermofisher Technology) instrument to collect the vibrational modes of functional groups within 400–4000 cm^{-1} wavelength. A differential scanning calorimeter (DSC) STA409PC (NETZSCH Scientific Instruments Trading Ltd.) was used operating at 20 °C to 800 °C under a nitrogen atmosphere at a scanning rate of 10 °C min^{-1}.

Scheme 1   Schematic of the (PAH/PSS)$_n$PAH microcapsules prepared *via* the layer–by–layer assembly.

Scheme 2   A combination of the crosslinker binding (PAH/PSS)$_n$PAH microcapsules with cotton fiber.

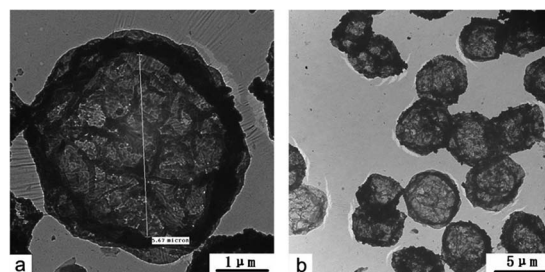Fig. 2   TEM images of (PAH/PSS)$_2$PAH.

2.4   Loading and release of Rhodamine B

(PAH/PSS)$_n$PAH microcapsules (2 mg mL^{-1}, 1.0 × 10^8) were washed and centrifuged with deionized water three times (7000 rpm min^{-1}, 1 min). Then, the washed microcapsules were incubated in the Rhodamine B (RhB) solution (2 mL, 1 mg mL^{-1}) at 25 °C for 24 hours. The RhB-loaded microcapsules were washed with PBS (pH 7.4) and centrifuged to calculate the loading efficiency (eqn 1-1). The release experiment of (PAH/PSS)$_n$PAH microcapsules was carried out in two buffers (pH 5.8 and pH 7.4) at 37 °C. The release process was performed as follows: RhB-loaded microcapsules were mixed with 4 mL of PBS (pH 5.8 and 7.4), 3 mL of supernatant was taken at different time intervals for absorbance measurements (λ = 554 nm, UV-1200 spectrophotometer, Mapada Instrument Co., Ltd.), and

then the supernatant was poured back into the initial solution. Finally, the cumulative release was calculated (eqn 1-2).

$$\text{Loading efficiency } (\%) = \frac{C_0 V_0 - C_1 V_1}{C_0 V_0} \times 100\% \qquad (1\text{-}1)$$

$$\text{Release rate } (\%) = \frac{C_t V_t}{C_0 V_0 - C_1 V_1} \times 100\% \qquad (1\text{-}2)$$

where C_0 (mg mL^{-1}) and V_0 (mL) are the initial concentration and volume of the RhB solution, respectively, C_1 (mg mL^{-1}) and V_1 (mL) are the concentration and volume of the RhB solution after incubation of microcapsules, respectively, and C_t (mg mL^{-1}) and V_t (mL) are the concentration and volume of the RhB solution at different time intervals during the release process.
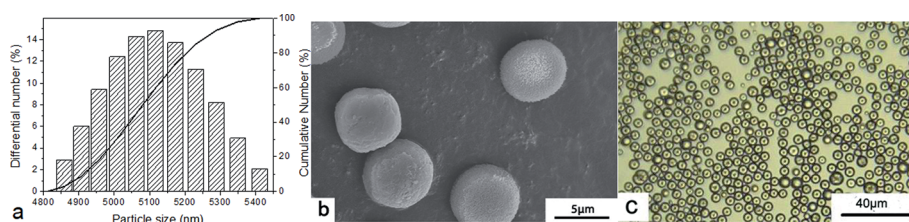

Fig. 1   Particle size distribution (a) SEM images (b) and optical images (c) of the CaCO$_3$ template.
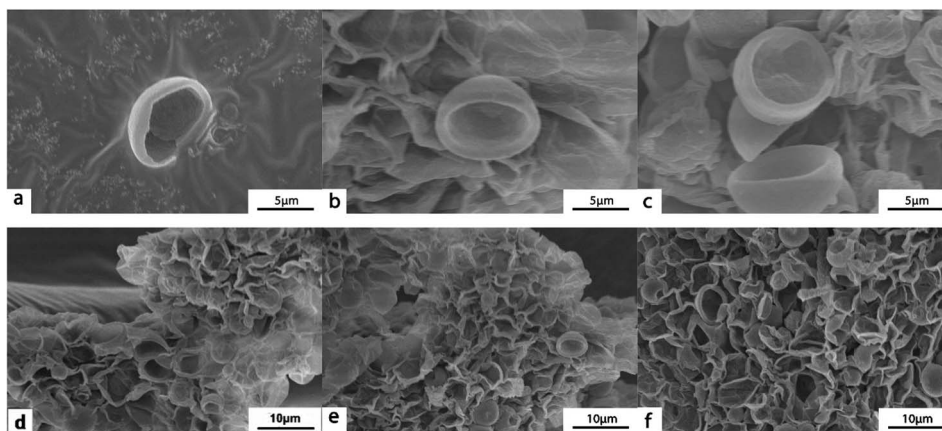
Fig. 3   SEM images of microcapsules with different layers: (a and d) (PAH/PSS)$_1$PAH; (b and e) (PAH/PSS)$_2$PAH; (c and f) (PAH/PSS)$_3$PAH.

The concentration can be calculated through the absorbance value and calibration curve.

2.5   Coating (PAH/PSS)$_n$PAH microcapsules on fabrics

The cotton fabrics (5 cm × 5 cm) were washed three times with deionized water and then were immersed into a 10 mL (PAH/PSS)$_n$PAH microcapsule suspension with different numbers of microcapsules shaking for 30 min. A positively charged compound with ethylene oxide groups used as a crosslinker was also added into the suspension to bind the microcapsules with cotton fibers. The combination of crosslinker, microcapsules and cotton fabrics is illustrated below (Scheme 2). Fabrics were then washed three times with deionized water and dried. After that, the properties of microcapsule-coated cotton fabrics were tested. And the coating percentage was calculated as follows:

$$\text{Coating percentage} (\%) = \frac{N_0 - N_i}{N_0} \qquad (1\text{-}3)$$

where N_0 was the initial microcapsules number added in the system, and N_i is the microcapsules number in the system after coating it on the cotton fabric.

3   Results and discussion

3.1   PSS-doped CaCO$_3$ particle characterization

During the process of forming the (PAH/PSS)$_n$PAH microcapsules, the CaCO$_3$ template plays an important role in determining their shape and the central cavity. As the polyelectrolyte PAH and PSS molecules self-assemble on the CaCO$_3$ template
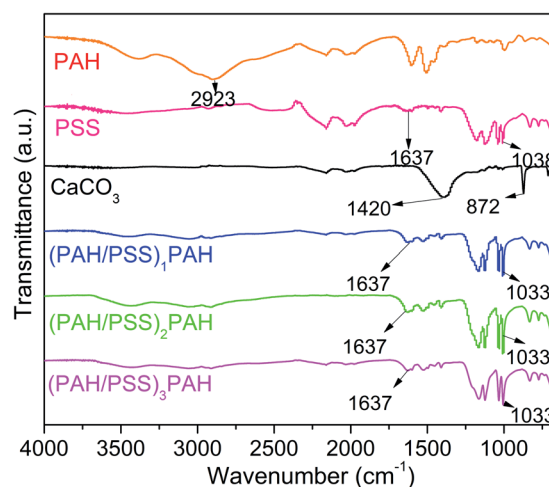

Fig. 5   FTIR spectra of (PAH/PSS)$_n$PAH microcapsules with different layers.

and form membranes with sizes at the micrometer level, the size of the CaCO$_3$ template determines the size of the microcapsules directly. The size distribution (Fig. 1a) showed that the CaCO$_3$ templates ranged in size from 4 μm to 6 μm: D (10%) = 4913.10 nm, D (50%) = 5080.70 nm, D (90%) = 5297.10 nm, which was suitable for forming the microcapsules. The scanning electron microscopy (SEM) and optical microphotographs of the formed PSS-CaCO$_3$ particles (Fig. 1b and c) displayed a typical structure of polycrystalline vaterite spheroids. These
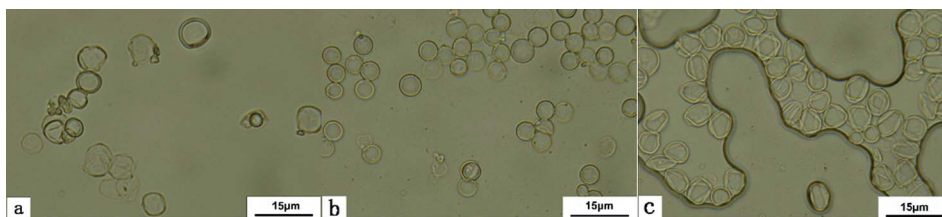

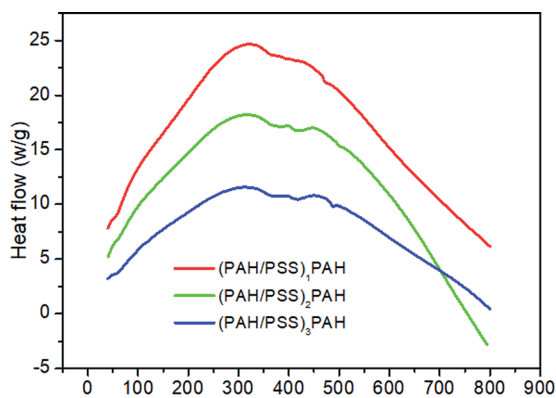Fig. 4   Optical images of microcapsules with different layers: (a) (PAH/PSS)$_1$PAH; (b) (PAH/PSS)$_2$PAH; (c) (PAH/PSS)$_3$PAH.

Fig. 6 DSC curves of (PAH/PSS)$_n$PAH microcapsules with different layers.

Fig. 8 SEM images of (PAH/PSS)$_2$PAH microcapsule-coated cotton fabrics with different microcapsule numbers: (a) 3.0×10^7; (b) 4.0×10^7; (c) 5.0×10^7; (d) 6.0×10^7.

particles afforded the advantages of PSS dispersion generating a smooth and regular surface.[43] This may be because the morphology of the products was affected by the strong interactions between the sulfonic groups of PSS and the Ca^{2+} ions, which influenced the nucleation and growth velocity on the $CaCO_3$ particles. Simultaneously, the addition of PSS yielded negative charges on the particle surface, which provided a structural basis for further assembly.

3.2 Preparation of (PAH/PSS)$_n$PAH microcapsules

PAH and PSS were employed to form microcapsules via the layer-by-layer (LBL) assembly driven by electrostatic interactions. The positively charged polyelectrolyte PAH was first coated on the surface of the PSS-doped $CaCO_3$ template (negatively charged due to PSS). Then, the negatively-charged PSS was coated on the resulting particles. By repeating the same coating process, multilayer coatings were formed. The $CaCO_3$ templates were etched by EDTA to obtain hollow microcapsules with different numbers of layers, (PAH/PSS)$_1$PAH, (PAH/PSS)$_2$PAH and (PAH/PSS)$_3$PAH, which can be briefly denoted as (PAH/PSS)$_n$PAH. The outermost layer of these microcapsules is positively charged PAH, providing suitable bonding with the cotton fabric (negatively charged cellulose fiber in an aqueous solution). The hollow structure of microcapsules serves as the reservoir for loading functional chemicals, e.g., dyes, drugs and perfumes. Moreover, composites formed by the oppositely charged polyelectrolytes usually exhibit pH responsibility because of the electrostatic interactions.[32–34] Thereby, (PAH/
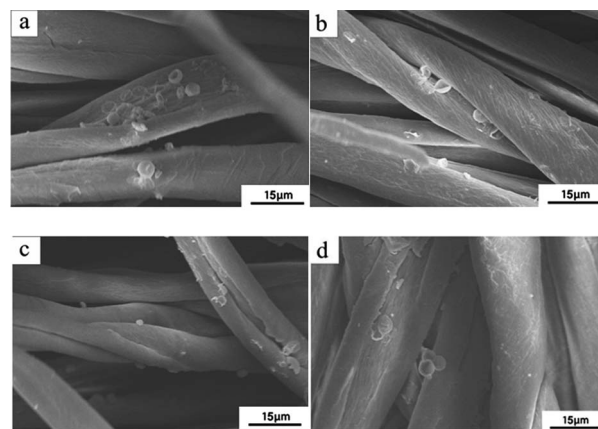
PSS)$_n$PAH microcapsules are supposed to be suitable materials for coating on the cotton fabric to manufacture the stimulus-responsive textiles, e.g., the pH-sensitive textiles with controlled-release triggered by human sweat.

3.3 Morphology of (PAH/PSS)$_n$PAH microcapsules

The morphology of (PAH/PSS)$_2$PAH can be seen in the transmission electron microscopy (TEM) images (Fig. 2). Microcapsules with different layers were prepared with a diameter of 4–6 μm. The TEM images show that PSS can mix with another polyelectrolyte PAH to form a stable structure of the microcapsules. This stable shell can prevent drug leakage. The SEM studies showed that the composite microcapsules (PAH/PSS)$_n$PAH had a spherical morphology, and became shriveled and plicate after drying. The SEM images confirm the presence of the hollow structures, with the visible collapse of the shells of the microcapsules during the drying process (Fig. 3). The diameters of the microcapsules indicated in the SEM images and optical images (Fig. 4) were 4–6 μm, corroborating the TEM results.

3.4 Structure of (PAH/PSS)$_n$PAH microcapsules

The FTIR spectra of PAH, PSS, $CaCO_3$, (PAH/PSS)$_1$PAH, (PAH/PSS)$_2$PAH and (PAH/PSS)$_3$PAH are presented in Fig. 5. The peaks in the region 3450–3420 cm^{-1} were due to the N–H groups, and the peaks in the region 1690–1620 cm^{-1} were due to the
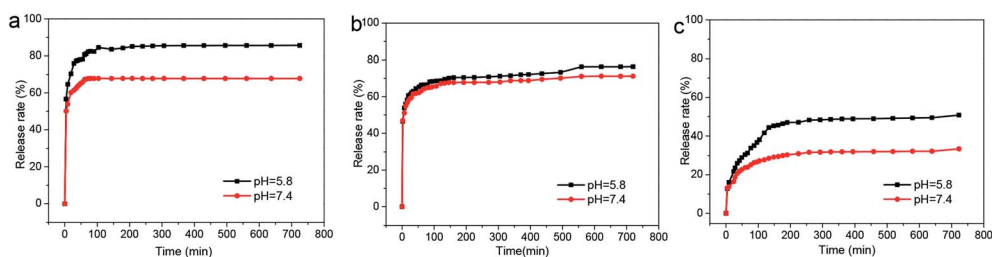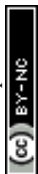

Fig. 7 RhB release from microcapsules with different layers at pH = 5.8 and 7.4. (a) (PAH/PSS)$_1$PAH; (b) (PAH/PSS)$_2$PAH; (c) (PAH/PSS)$_3$PAH.
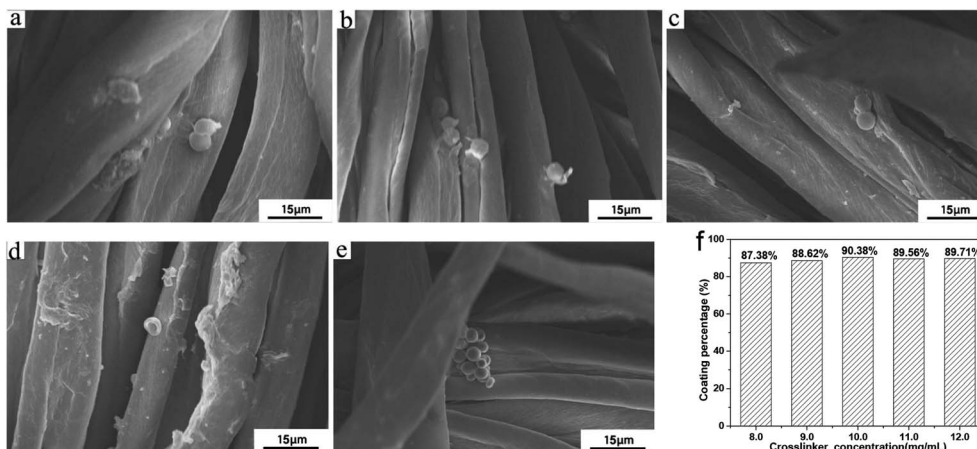
Fig. 9 SEM images of (PAH/PSS)$_2$PAH microcapsule-coated cotton fabric with different concentrations of the crosslinker: (a) 8.0 mg mL^{-1}; (b) 9.0 mg mL^{-1}; (c) 10.0 mg mL^{-1}; (d) 11.0 mg mL^{-1}; (e) 12.0 mg mL^{-1}; (f) coating percentages microcapsules on cotton fabric at different concentrations of the crosslinker. The initial microcapsules added into the system were 1.0×10^8.

stretching vibrations of C=O. An intensive absorption band at 872 cm^{-1} corresponded to the CO$_3^{2-}$ and the band observed at 1420 cm^{-1} was the stretching vibration of C–O. The main bands of PSS were assigned to the 1038 cm^{-1} peak due to the S–O stretching vibration deformation and the symmetric stretching of the S=O peak at 1123 cm^{-1} in Fig. 5. The peak at 2923 cm^{-1} was due to the asymmetric vibration of the –CH$_2$ groups of PAH-Cl. The presence of the protonated NH^{3+} groups in PAH-Cl species was confirmed from the bands related to the asymmetric vibrations of these species that can be observed at 1512–1637 cm^{-1}. As shown in Fig. 5, these peaks corresponded to the (PAH/PSS)$_n$PAH microcapsules, indicating the successful interaction of PAH and PSS into the microcapsule structures and the removal of the CaCO$_3$ template.[44–46]

3.5 DSC analysis of (PAH/PSS)$_n$PAH microcapsules

As shown in Fig. 6, microcapsules with different numbers of layers, (PAH/PSS)$_1$PAH, (PAH/PSS)$_2$PAH and (PAH/PSS)$_3$PAH were also characterized *via* differential scanning calorimetry (DSC), to investigate their thermal properties. The stage around 60 °C to 300 °C is attributed to the evaporation of absorbed and combined water.[47,48] In general, the decomposition of polymers requires a higher temperature. The peak at 300 °C to 500 °C represents the decomposition and degradation of PAH and PSS, since a typical temperature to induce the thermal degradation of ordinary carbon polymers is about 400–500 °C.[47] This result confirms the stable thermal behavior of the (PAH/PSS)$_n$PAH microcapsules, allowing its wide applications as functional materials.

3.6 Release of RhB

It is well known that the pH of the body surface is nearly neutral and will decrease to weakly acidic as sweating proceeds. In this study, the efficiency of microcapsules with a single layer, double layers and triple layers is 76.82%, 74.72% and 66.16%, respectively. As shown in Fig. 7, the test analysis showed that the

releases of RhB from the same layered (PAH/PSS)$_n$/PAH microcapsules at pH 7.4 and pH 5.8 were significantly different. The release efficiency at pH 5.8 was much higher than that at pH 7.4. That could be due to the protonation of PSS and PAH in the acidic buffer solution, so that the wall structure consisting of a composite film became loose and its permeability was enhanced. For up to 600 min, the (PAH/PSS)$_1$/PAH, (PAH/PSS)$_2$/PAH and (PAH/PSS)$_3$/PAH microcapsules prepared with increasing numbers of PAH/PSS layers at pH 7.4 showed the release percentages of 66.17%, 61.32%, 53.18%, respectively, while at pH 5.8 the release percentages were 72.11%, 69.68%, 63.09%, respectively, which are much higher than those at pH 7.4. Besides, the release of RhB from the microcapsules decreases with the increase in the number of assembly layers. It is known that the permeation behavior is closely related to the thickness of the microcapsule shell formed by PAH and PSS. The more number of layers would increase the route distance and blocking effect for RhB dispersing out of microcapsule, reducing the release percentage.[49] This can also explain why the (PAH/PSS)$_1$/PAH microcapsules showed faster release than the (PAH/PSS)$_3$PAH microcapsules.

3.7 (PAH/PSS)$_2$PAH microcapsules coated on cotton fabric

As a carrier on a material, microcapsules can exhibit good pH stimulus releasing performance (Fig. 7). Therefore, an embedded chemical such as drugs or perfumes can functionalize a fabric with stimulus-responsive controlled release property. Here (PAH/PSS)$_2$PAH microcapsules were combined with a cotton fabric to obtain a controlled releasing textile. On the outermost surface of the (PAH/PSS)$_2$PAH microcapsules, the amino group from PAH provided a positive charge. Therefore, under near-neutral conditions, due to the electrostatic forces, the (PAH/PSS)$_2$PAH microcapsules can combine with the cellulose fibers, which are negatively charged because of the hydroxyl groups. The SEM images of the fabrics treated with different quantities of microcapsules ($3.0–6.0 \times 10^7$) are shown in Fig. 8. Also, with the increase in the number of treatments, the

number of coated microcapsules increased as follows, 2.17×10^7 (3.0×10^7), 2.85×10^7 (4.0×10^7), 3.53×10^7 (5.0×10^7) and 4.01×10^7 (6.0×10^7). However, the coating percentage decreased with the increase in the number of added micro-capsules (from 72.35% to 66.72% with respect to the initial addition of microcapsules of 3.0×10^7 to 6.0×10^7). This might relate to the competition of microcapsules. Therefore, it was necessary to introduce some agents that worked as crosslinkers for bonding the microcapsules with the cotton fiber more effectively.

In order to improve the efficient interaction between the $(PAH/PSS)_2PAH$ microcapsules and cotton fabric, a positively charged compound with ethylene oxide groups was used as a crosslinker to bind $(PAH/PSS)_2PAH$ microcapsules with cotton fibers firmly. The effect of the crosslinker on the microcapsule coating percentage on the cotton fabric is shown in Fig. 9. The coating percentage increased with the increase in the concen-tration of the crosslinker (from 87.38% to 90.38%) at an initial number of microcapsules of 1.0×10^8. The positively charged part NR_4^+ of the crosslinker was bonded with $-COO^-$ ($-COOH$) or $-O^-$ ($-OH$) groups of the cotton fiber and the ethylene oxide groups interacted with the $-NH_3^+$ group of the outermost layer PAH of the $(PAH/PSS)_2PAH$ microcapsules. In this way, $(PAH/PSS)_2PAH$ microcapsules could be coated on the cotton fibers more efficiently.

4 Conclusion

In this study, the polyelectrolytes PAH and PSS were assembled on the $CaCO_3$ template by the LBL self-assembly. Then, the template was removed to yield the hollow composite micro-capsules. The results showed that the particle size of the $CaCO_3$-templated microcapsule ranged from 4–6 μm. Through the SEM and TEM studies, the hollow structure of the composite microcapsules was confirmed and the size of the microcapsules was 4–6 μm. The FTIR spectra showed that the polyelectrolytes PAH and PSS were incorporated to form the microcapsules *via* electrostatic binding. The resulting composite hollow micro-capsules were used to study the loading and release of RhB under different conditions. The release rate for RhB was closely related to the number of layers of the hollow microcapsules. As the microcapsules were responsive to pH, the rate of the RhB release varied with pH, and it was higher at pH 5.8 than at pH 7.4. In this study, $(PAH/PSS)_2PAH$ microcapsules as a carrier were used for coating on the cotton fabrics to introduce func-tional chemicals into the textile. Under neutral conditions, PAH/PSS microcapsules could be combined with cotton fiber through $-NH_3^+$ of PAH and $-O^-$ ($-OH$) or $-COO^-$ ($-COOH$) of cotton cellulose molecules. Besides, a positively charged compound with ethylene oxide groups was added as a cross-linker between $(PAH/PSS)_2PAH$ microcapsules and the cotton fibers. The bonding effect of this crosslinker enhanced the combination of microcapsules with the cotton fiber. With the increasing amount of the crosslinker, the coating percentage of microcapsules on the cotton fabric increased. Since the inter-action between PAH and PSS was sensitive to pH, this $(PAH/PSS)_nPAH$ microcapsule-coated fabric can be employed as a pH

stimulus-responsive textile, releasing functional chemicals with the changes of the surrounding environment. Moreover, this microcapsule-coating modification on fabrics could introduce various chemicals, *e.g.*, drugs, natural herbs, perfumes, into common fabrics to obtain functional textiles with long-lasting releasing effects. The LBL microcapsules can be formed by different assemble blocks and be combined with fabrics. Using materials with different properties to prepare the LBL micro-capsules and then coating on fabrics, functional textiles with various stimulus-responsivity can be obtained. This work can provide a potential technique to design stimulus-responsive textiles for applications in many areas.

Conflicts of interest

There are no conflicts of interest to declare.

Acknowledgements

References

1 X. Wu, X. Wang, W. Lu, X. Wang, J. Li, H. You, H. Xiong and L. Chen, *J. Chromatogr. A*, 2016, **1435**, 30–38.
2 M. A. C. Stuart, W. T. S. Huck, J. Genzer, M. Müller, C. Ober, M. Stamm, G. B. Sukhorukov, I. Szleifer, V. V. Tsukruk, M. Urban, F. Winnik, S. Zauscher, I. Luzinov and S. Minko, *Nat. Mater.*, 2010, **9**, 101–113.
3 L. Xiao, A. B. Isner, J. Z. Hilt and D. Bhattacharyya, *J. Appl. Polym. Sci.*, 2013, **128**, 1804–1814.
4 J. Liu, Y. Huang, A. Kumar, A. Tan, S. Jin, A. Mozhi and X. Liang, *Biotechnol. Adv.*, 2014, **32**, 693–710.
5 H. Zheng, Y. Zhang, L. Liu, W. Wan, P. Guo, A. M. Nyström and X. Zou, *J. Am. Chem. Soc.*, 2016, **138**, 962–968.
6 J. Zhuang, C. Kuo, L. Chou, D. Liu, E. Weerapana and C. Tsung, *ACS Nano*, 2014, **8**, 2812–2819.
7 Z. Zhang and N. Hadjichristidis, *ACS Macro Lett.*, 2018, **7**, 886–891.
8 J. L. Vivero Escoto, I. I. Slowing, B. G. Trewyn and V. S. Y. Lin, *Small*, 2010, **6**, 1952–1967.
9 Y. Cheng, K. Ren, D. Yang and J. Wei, *Sens. Actuators, B*, 2018, **255**, 3117–3126.
10 S. S. Lee and S. Kim, *Macromol. Res.*, 2018, **26**, 1054–1065.
11 J. M. Korde and B. Kandasubramanian, *Ind. Eng. Chem. Res.*, 2019, **58**, 9709–9757.
12 A. Khalaj Asadi, M. Ebrahimi and M. Mohseni, *Pigm. Resin Technol.*, 2017, **46**, 318–326.
13 K. Iqbal and D. Sun, *Cellulose*, 2018, **25**, 2103–2113.
14 D. Štular, I. Jerman, B. Simončič, K. Grgić and B. Tomšič, *Cellulose*, 2018, **25**, 6231–6245.

15 M. I. Guignard, C. Campagne, S. Giraud, M. Brebu, N. Vrinceanu and L. Cioca, *Sens. Actuators, B*, 2015, **106**, 119–132.

16 T. Yan, X. Chen, T. Zhang, J. Yu, X. Jiang, W. Hu and F. Jiao, *Chem. Eng. J.*, 2018, **347**, 52–63.

17 C. Massaroni, P. Saccomandi, D. Formica, D. Lo Presti, M. A. Caponero, G. Di Tomaso, F. Giurazza, M. Muto and E. Schena, *IEEE Sens. J.*, 2016, **16**, 8103–8110.

18 A. P. Esser-Kahn, S. A. Odom, N. R. Sottos, S. R. White and J. S. Moore, *Macromolecules*, 2011, **44**, 5539–5553.

19 D. Sun, G. Sun, X. Zhu, A. Guarin, B. Li, Z. Dai and J. Ling, *Adv. Colloid Interface Sci.*, 2018, **256**, 65–93.

20 A. Sharkawy, I. P. Fernandes, M. F. Barreiro, A. E. Rodrigues and T. Shoeib, *Ind. Eng. Chem. Res.*, 2017, **56**, 5516–5526.

21 B. M. Wohl and J. F. J. Engbersen, *J. Controlled Release*, 2012, **158**, 2–14.

22 S. Correa, E. C. Dreaden, L. Gu and P. T. Hammond, *J. Controlled Release*, 2016, **240**, 364–386.

23 Z. Zhang, S. Zhang, R. Su, D. Xiong, W. Feng and J. Chen, *J. Food Sci.*, 2019, **84**, 1427–1438.

24 M. B. Thomas, M. Vaidyanathan, K. Radhakrishnan and A. M. Raichur, *J. Food Eng*, 2014, **136**, 1–8.

25 D. Luo, R. N. Poston, D. J. Gould and G. B. Sukhorukov, *Mater. Sci. Eng. C*, 2019, **94**, 647–655.

26 S. De Koker, B. G. De Geest, C. Cuvelier, L. Ferdinande, W. Deckers, W. E. Hennink, S. C. De Smedt and N. Mertens, *Adv. Funct. Mater.*, 2007, **17**, 3754–3763.

27 L. Zhang, Y. Wang, N. Tang, P. Cheng, J. Xiang, W. Du and X. Wang, *React. Funct. Polym.*, 2016, **99**, 73–79.

28 E. Dellacasa, L. Zhao, G. Yang, L. Pastorino and G. B. Sukhorukov, *Beilstein J. Nanotechnol.*, 2016, **7**, 81–90.

29 S. Anandhakumar, P. Gokul and A. M. Raichur, *Mater. Sci. Eng. C*, 2016, **58**, 622–628.

30 D. Luo, S. Shahid, R. M. Wilson, M. J. Cattell and G. B. Sukhorukov, *ACS Appl. Mater. Interfaces*, 2016, **8**, 12652–12660.

31 W. Zhang, L. Deng, G. Wang, X. Guo, Q. Li, J. Zhang and N. M. Khashab, *Part. Part. Syst. Charact.*, 2014, **31**, 985–993.

32 W. Zhou, Z. Jia, P. Xiong, J. Yan, M. Li, Y. Cheng and Y. Zheng, *Mater. Sci. Eng. C*, 2018, **90**, 693–705.

33 J. Sun, C. Su, X. Zhang, J. Li, W. Zhang, N. Zhao, J. Xu and S. Yang, *J. Colloid Interface Sci.*, 2018, **513**, 470–479.

34 D. Alemu, H. Wei, K. Ho and C. Chu, *Energy Environ. Sci.*, 2012, **5**, 9662–9671.

35 C. Sung and J. L. Lutkenhaus, *Korean J. Chem. Eng.*, 2018, **35**, 263–271.

36 C. Huang and F. Chang, *Macromolecules*, 2009, **42**, 5155–5166.

37 C. Chen, G. Chen, P. Wan, D. Chen, T. Zhu, B. Hu, Y. Sun and X. Zeng, *J. Agric. Food Chem.*, 2018, **66**, 11141–11150.

38 F. Khan, P. Liu, F. Xu, Y. Ma and Y. Qiu, *RSC Adv.*, 2016, **6**, 20286–20293.

39 K. Chen, C. Xu, J. Zhou, R. Zhao, Q. Gao and C. Wang, *Carbohydr. Polym.*, 2020, **232**, 115821.

40 A. Bashari, N. Hemmatinejad and A. Pourjavadi, *IEEE Trans. NanoBioscience*, 2017, **16**, 455–462.

41 Z. Zhang, M. Azizi, M. Lee, P. Davidowsky, P. Lawrence and A. Abbaspourrad, *Lab Chip*, 2019, **19**, 3448–3460.

42 L. Manjakkal, S. Dervin and R. Dahiya, *RSC Adv.*, 2020, **10**, 8594–8617.

43 S. L. Yefimova, I. I. Bespalova, G. V. Grygorova, A. V. Sorokin, P. V. Mateychenko, X. Q. Cui and Y. V. Malyukin, *Microporous Mesoporous Mater.*, 2016, **236**, 120–128.

44 G. K. Such, A. P. R. Johnston and F. Caruso, *Chem. Soc. Rev.*, 2011, **40**, 19–29.

45 K. Murugan, A. Jaganathan, R. Rajaganesh, U. Suresh, J. Madhavan, S. Senthil-Nathan, A. Rajasekar, A. Higuchi, S. S. Kumar, A. A. Alarfaj, M. Nicoletti, R. Petrelli, L. Cappellacci, F. Maggi and G. Benelli, *J. Cluster Sci.*, 2018, **29**, 27–39.

46 S. Balu, M. V. Sundaradoss, S. Andra and J. Jeevanandam, *Beilstein J. Nanotechnol.*, 2020, **11**, 285–295.

47 W. Tong and C. Gao, *Polym. Adv. Technol.*, 2005, **16**, 827–833.

48 F. Göktepe, A. Bozkurt and Ş. T. Günday, *Polym. Int.*, 2008, **57**, 133–138.

49 M. Akbar, E. Cagli and I. Erel-Göktepe, *Macromol. Chem. Phys.*, 2019, **220**, 1800422.